Paroxysmal Atrial Fibrillation Caused by Interaction of Pacemaker Waves and Reduced Excitability: Insights from the Bueno-Orovio Model Adapted to Atria

Claudia Lenk[1], Frank M Weber[2,3], Martin Bauer[2], Mario Einax[4], Gunnar Seemann[2], Philipp Maass[4]

[1] Institut für Chemie und Biotechnik, Technische Universität Ilmenau, Ilmenau, Germany
[2] Institute of Biomedical Engineering, Karlsruhe Institute of Technology, Karlsruhe, Germany
[3] Philips Research Europe, Hamburg, Germany
[4] Fachbereich Physik, Universität Osnabrück, Osnabrück, Germany

Abstract

As possible cause for atrial fibrillation (AF) we study the influence of a reduced excitability on the interaction of pacemaker waves in the Bueno-Orovio model with parameters adapted to atrial electrophysiology (aBO). One of the two pacemakers represents the sinus node and the other one a self-excitatory source in the left atrium. The pacemakers are spatially separated and their waves get in contact via a small bridge. In previous studies based on the FitzHugh-Nagumo (FHN) model it was shown that three different types of irregular activation patterns can occur in this problem. In the aBO model adapted to physiological conditions only one type is observed because, different from the FHN model, a reduction of excitability due to high-frequency pacing does not occur. If the excitability is reduced in the aBO model, all types of irregularities are recovered and, in addition, a further type is found. Because transitions from regular to irregular behavior depend on the pacing frequency, our findings provide a possible explanation for the phenomenon of paroxysmal AF.

1. Introduction

Atrial fibrillation (AF) is a cardiac disease with irregular and fast activation of the atria [1]. This can lead to symptoms like palpitations, chest discomfort and lightheadedness. Additionally, AF can lead to the formation of blood clots due to incomplete atrial contraction. AF normally starts with short, self-terminating periods and progresses to longer and more frequent episodes due to electrical and structural remodeling of the atrial tissue. Recently, some of us suggested [2] that a possible reason for paroxysmal AF lies in an interaction of waves emanating from two pacemakers, where the primary one with frequency $f_{\rm pace}$ represents the sinus node in the right atrium, and the secondary one with perturbation frequency $f_{\rm pert}$ represents a self-excitatory source in the left atrium. The latter can be an ectopic focus or spiral wave, as often observed in the left atrium [3]. Using the FHN model [4], it was shown that the interaction can yield three different types of fibrillation-like patterns that occur in distinct regions of the $f_{\rm pace} - f_{\rm pert}$ plane.

For the BO model [5] adapted to atrial electrophysiology (aBO) [6], only one type of irregular pattern was observed and this with reduced strength compared to the FHN model [7]. Different from the FHN model, restitution properties of the aBO model inhibit a reduction of excitability due to high-frequency pacing. In order to see whether a reduction of the excitability can have similar effects in the BO model, we here study the interaction of pacemaker waves in the aBO model with parameters yielding a reduced excitability (aBO-re variant).

2. Model

The Bueno-Orovio model [5] describes action potential (AP) generation and propagation in ventricular tissue without including detailed microscopic dynamics of ion channels, pumps and exchangers. The basic evolution equation for the membrane voltage equivalent u is

$$\partial_t u \;=\; D\nabla^2 u - \left(J_{\rm fi} + J_{\rm so} + J_{\rm si} + J_{\rm extern}\right), \quad (1)$$

where $J_{\rm fi}$ is the fast inward current, $J_{\rm si}$ the slow inward current, $J_{\rm so}$ the slow outward current and $J_{\rm extern}$ an external stimulus. These currents are controlled by three gating variables s, v, and w, which follow relaxation equations of Hodgkin-Huxley type. The gating variable v controls the fast inward current $J_{\rm fi}$, whereas the slow outward current $J_{\rm so}$ depends on u only. The slow inward current $J_{\rm si}$ is governed by two gating variables, namely w for the restitution behavior and s for the spike-and-dome morphology of the action potential. The complete equations of the BO model are given in Ref. [5], and parameters for application to the atria (aBO model) were determined in Ref. [5], such that the AP, conduction velocity (CV) and restitution curves re-

semble that of the Courtemanche model [8]. For the aBO-re variant the relaxation time τ_{fi} of J_{fi} is increased from 0.045 to 0.062. This does not change AP shape or CV but the maximal pacing frequency is reduced from 3.03 Hz in the aBO model to 2.7 Hz in aBO-re variant. For pacing frequencies larger than this frequency, waves propagate only at every second pulse.

Calculations are carried out for a simulation geometry of size 21×10 (length unit is 1 cm) as shown fig. 1. The simulation area is divided into three regions: the rectangular region L with $0 \leq x \leq 10$, $0 \leq y \leq 10$ representing the left atrium, the rectangular region R with $11 \leq x \leq 21$, $0 \leq y \leq 10$, representing the right atrium, and the small bridge B with $10 < x < 11$, $4 < y < 6$ representing the fast conducting pathways (e.g. Bachmann's bundle) between the electrically isolated atria. No-flux conditions are applied to all boundaries in fig. 1. The primary pacemaker

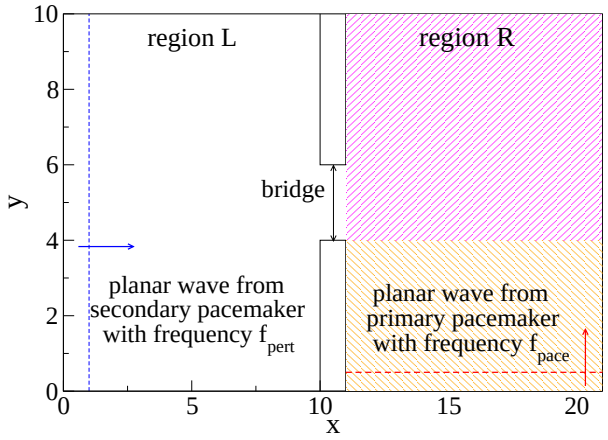

Figure 1. Sketch of the simulation area with the two pacemakers.

generates waves in the stripe $11 \leq x \leq 21$, $y \leq 0.02$ by application of an external current with amplitude 0.01 A, duration 50 ms, and frequency f_{pace}. The secondary waves are generated by application of an external current with amplitude 0.01 A, duration 50 ms, and frequency f_{pert} in the stripe $x \leq 0.02$, $0 \leq y \leq 10$. For solving the set of differential equations the cardiac simulation tool acCELLerate [9] was used with time step of $5\,\mu$s and 2100×1000 voxels having a resolution of 0.01 cm.

Irregularity of the patterns is quantified by an order parameter

$$\Phi = \frac{2}{N_g(N_g-1)} \sum_{j>k}^{N_g} \left| \langle \exp[i(\Delta\varphi_{jk}(t)] \rangle_t \right|, \qquad (2)$$

for phase coherence [10] in region R. Here, N_g is the number of grid points in R, $\Delta\varphi_{jk}(t) = \varphi_j(t) - \varphi_k(t)$ is the time-dependent phase difference, and $\langle \ldots \rangle_t$ denotes a time average. The phase φ_j at point j is calculated from $u_j(t)$ by the analytic signal approach, detailed in Ref. [2]. For regular excitation patterns with one frequency, Φ is close to one, while irregular activation patterns, showing reentrant waves, wave fragments or wave breaks, lead to Φ values smaller than one.

3. Results

As mentioned above, the interaction of pacemaker waves can give rise to different types of irregular patterns dependent on f_{pace} and f_{pert}. Type I refers to the detachment of primary waves from the lower right boundary of the bridge. Subsequent curling of the resulting open end of the wavefront and interaction with the secondary waves leads to irregular patterns. Without reduction of excitability, this type of irregularity occurs only in the FHN model and if f_{pace} is larger than the critical frequency f_c^{FHN}, where waves detach from corners. In the aBO model, type I is not observed, but in the aBO-re variant it appears, if $f_{\mathrm{pert}} < f_{\mathrm{pace}}$ (and $f_{\mathrm{pace}} < f_c^{\mathrm{BO}}$, see below).

Type II is caused by the detachment of the secondary waves from the corners at the right-hand side of the bridge. A curling of the resulting wavefront ends occurs, which can lead to two counterrotating spirals in region R. If these are disturbed by the primary waves, irregular patterns arise. In the FHN model type II is observed for $f_{\mathrm{pert}} > f_c^{\mathrm{FHN}}$ and $f_{\mathrm{pace}} < f_c^{\mathrm{FHN}}$. It is always present in the aBO-re variant as long as $f_{\mathrm{pert}} < f_c^{\mathrm{BO}}$.

Type III occurs in both, the FHN and the aBO model, as well as in the aBO-re variant for $f_{\mathrm{pert}} > f_{\mathrm{pace}}$. In this case secondary waves expel the primary ones, pass the bridge and become circular wavefronts in region R. The primary waves generated at the lower part of region R can partially penetrate into the space between the circular wavefronts. As a consequence wave fragments are build in a small area close to the lower boundary in region R.

Type IV irregularity occurs in the aBO-re variant for f_{pert} exceeding a critical frequency f_c^{BO}, where conduction of the secondary waves is partially blocked at the bridge. The subsequent secondary wave can pass the bridge normally and form a circular wavefront in region R, corresponding to a "regular 2:1 block". However, it is also possible that the subsequent secondary wave following a block is strongly disturbed and appears as a small wave fragment in region R. If a fragment appears, the behavior of the following secondary waves is not predictable. Further wave fragments can be generated in region R or the secondary waves can get blocked again.

The wave fragments appearing in region R either dissipate or grow. In the latter case the ends of the wavefront become curled and, because of perturbation with the primary waves, irregular patterns with stable reentry or wave breaks evolve. A typical example for a growing wave fragment is shown in fig. 2 for $f_{\mathrm{pace}} = 3.03$ Hz and

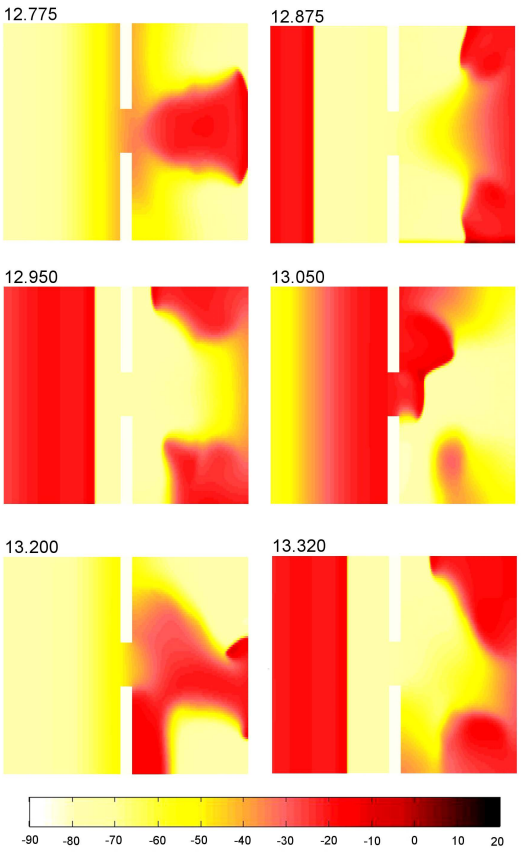

Figure 2. Time evolution of transmembrane voltage for $f_{\mathrm{pace}} = 3.03$ Hz and $f_{\mathrm{pert}} = 2.5$ Hz in the aBO-re variant. Red color represents the excited state, yellow the excitable or refractive state. Numbers above graphs give the time instant in seconds.

$f_{\mathrm{pert}} = 2.5$ Hz. At time $t = 12.775$ s, the initial pattern is displayed. At $t = 12.875$ s the open ends of the wavefront are curled and a primary wave is generated, as it can be seen from the thin stripe appearing at the lower boundary of region R. The left part of the primary wave can not propagate because the preceding wave fragment has brought the tissue near the bridge into the refractory state. The primary wave disturbs the propagation of the lower end of the curled secondary wavefront ($t = 12.95$ s). This perturbation yields the dissipation of the lower part of the curled wavefront ($t = 13.05$ s). Around the same time another secondary wave passes the bridge. Together with the upper end of the curled wavefront a stable reentrant pattern is formed ($t = 13.2$ and 13.32 s).

Figure 3 shows, for the aBO-re variant, the occurrence of the different types of irregularities in the $f_{\mathrm{pace}} - f_{\mathrm{pert}}$ plane. If $f_c^{\mathrm{BO}} > f_{\mathrm{pert}} > f_{\mathrm{pace}}$ and f_{pert} is not a multiple of f_{pace}, irregular patterns are formed that are a mixture

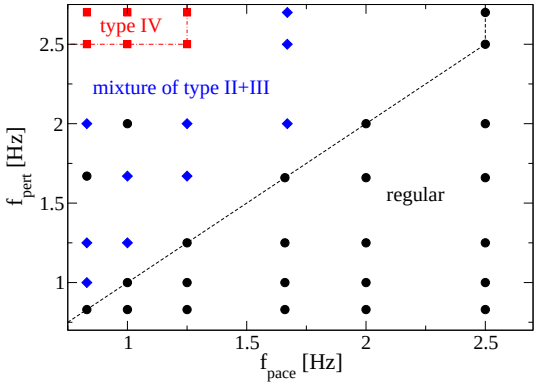

Figure 3. Occurrence of different types of irregularities in the $f_{\mathrm{pace}} - f_{\mathrm{pert}}$ plane for the aBO-re variant.

of type I, II and III. Detachment and irregularities of type I and II are observed for all frequencies smaller than f_c^{BO} and $f_{\mathrm{pace}} > f_{\mathrm{pert}}$. Because their strength, quantified by Φ, is small, we consider them as nearly regular here.

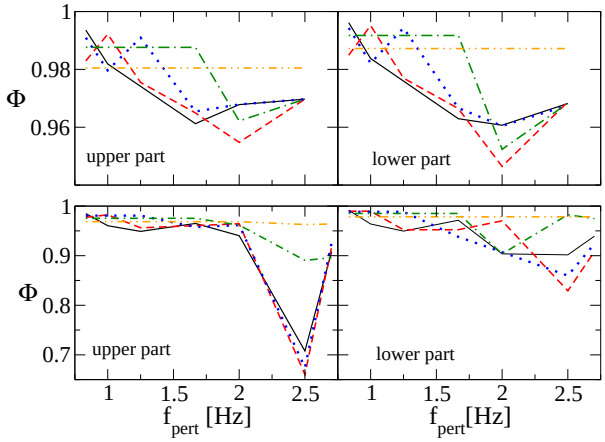

Figure 4. Phase coherence parameter Φ in dependence of f_{pert} calculated in regions $y > 4$ (upper part) and $y < 4$ (lower part) for $f_{\mathrm{pace}} = 0.83$ Hz (black solid line), 1 Hz (red dashed line), 1.25 Hz (blue dotted line), 1.67 Hz (green dash-dotted line), and 2.5 Hz (orange dot-dot-dashed line). The upper panels show the results for the aBO model and the lower panels for the aBO-re variant.

The parameter Φ is shown in fig. 4 as function of f_{pert} for various values of f_{pace}, both the aBO model (upper two panels) and the aBO-re variant (lower two panels). For $f_{\mathrm{pert}} < f_{\mathrm{pace}}$, Φ is close to one, indicating regular patterns, although detachment occurs in the aBO-re variant in this frequency range. If $f_{\mathrm{pert}} > f_{\mathrm{pace}}$ and both frequencies are smaller than f_c^{BO} (black, red and blue curve), Φ decreases slightly with rising f_{pert} in the aBO model and the aBO-re variant. This decrease is caused by the occurrence of type III irregularity. If $f_{\mathrm{pert}} > f_c^{\mathrm{BO}}$ and $f_{\mathrm{pace}} < f_c^{\mathrm{BO}}$,

a strong decrease of Φ is seen for the aBO-re variant due to type IV irregularity. For $f_{\mathrm{pace}} > f_c^{\mathrm{BO}}$ (orange dot-dot-dashed curve), Φ is unaffected by changes in f_{pert}, because the primary waves expel the secondary waves and generate irregular patterns in region L.

4. Conclusions

We showed that the interaction of pacemaker waves via a small bridge can yield irregular patterns in the aBO model and in the aBO-re variant, where the excitability is decreased by a slowing down of the fast-inward current. This reduction of excitability can arise in cardiac tissue as a result of, e.g., mutations [11]. In neuronal cells a reduction of excitability has recently been seen as a consequence of aging [12]. Type I and II irregularities, identified in the FHN model in a previous study, are also found in the aBO-re variant, but with a very small strength. To a lower extent this decrease of strength is observed also for type III irregularity in the aBO model and the aBO-re variant.

A further type IV of irregularity is found in the aBO-re variant, whose strength is much larger than that of the other types. It is initiated by a partial conduction block of the secondary waves at the bridge in the simulation geometry. It was shown by Cabo *et al.* [13], both in experiments with isolated sheep myocardium and in numerical calculations of the Luo-Rudy model, that a conduction block can arise from propagation of waves through a small isthmus. It was found that the critical size of the isthmus, for which conduction block occurs, depends on the frequency of the waves. For our simulations with a bridge width of 2 cm, the conduction block is not observed in the aBO model, but it may be seen in simulations with smaller bridge widths. Berenfeld *et al.* [14] showed that high-frequency pacing of Bachmann's bundle of isolated sheep right atrium can generate disorganized wave propagation comparable to fibrillation patterns. Comparable results are seen in our simulations for type II and IV irregularity in the aBO-re variant, although the critical frequency for the transition from regular to irregular wave propagation was higher.

The interaction of pacemaker waves as studied here can be a cause for AF initiation. Because transitions between regular and irregular patterns can be induced by a change of the frequencies of the two pacemakers, our findings provide a possible explanation for paroxysmal AF.

Acknowledgements

Claudia Lenk thanks the Carl-Zeiss-Stiftung for financial support. P. M. gratefully acknowledges financial support by the Deutsche Forschungsgemeinschaft (grant no. MA 1636/8-1).

References

[1] Camm AJ, Kirchhof P, Lip GYH, Schotten U, Savelieva I, Ernst S, Van Gelder IC, Al-Attar N, Hindricks G, Prendergast B, Heidbuchel H, Aleri O, Angelini A, Atar D, Colonna P, De Caterina R, De Sutter J, Goette A, Gorenek B, Heldal M, Hohloser SH, Kolh P, Le Heuzey J-Y, Ponikowski P, Rutten FH. Guidelines for the management of atrial fibrillation. European Heart Journal 2010;31:2369-2429.

[2] Lenk C, Einax M, Maass P. Irregular excitation patterns in reaction-diffusion systems due to perturbation by secondary pacemakers. Phys. Rev. E. 2013;87:042904-1–8.

[3] Sanders P, Berenfeld O, Hocini M, Jais P, Vaidyanathan R, Hsu LF, Garrigue S, Takahashi Y, Rotter M, Sacher F, Scavee C, Ploutz-Snyder R, Jalife J, Haisaguerre M. Spectral Analysis Identifies Sites of High-Frequency Activity Maintaining Atrial Fibrillation in Humans. Circulation 2005;112:789-797.

[4] FitzHugh R. Impulses and physiological states in theoretical models of nerve membrane. Biophys. J. 1995;1:445-466.

[5] Bueno-Orovio A, Cherry EM, Fenton FH. Minimal model of human ventricular action potentials in tissue. J. theo. Biol. 2008;253:544-560.

[6] Weber FM. Personalizing Simulations of the Human Atria: Intracardiac Measurements, Tissue Conductivities, and Cellular Electrophysiology. In: Karlsruhe Institute of Technology, Institute of Biomedical Engineering, editors. Karlsruhe Transactions on Biomedical Engineering 2011;12.

[7] Lenk C, Einax M, Seemann G, Maass P. Interaction of Pacemakers as Generating Mechanism of Atrial Fibrillation. CINC 2011;38:229-232.

[8] Courtemanche R, Ramirez RJ, Nattel S. Ionic mechanisms underlying the human atrial action potential properties: insights from a mathematical model. Am. J. Physiol. 1998;275:H301–21.

[9] Seemann G, Sachse FB, Karl M, Weiss DL, Heuveline V, Dössel O. Framework for Modular, Flexible and Efficient Solving the Cardiac Bidomain Equations Using PETSc. In: Fitt AD, Progress in Industrial Mathematics at ECMI 2008. Mathematics in Industry 2010;15:363–9.

[10] Taylor AF, Kapetanopoulos P, Whitaker BJ, Toth R, Bull L, Tinsley MR. Phase clustering in globally coupled photochemical oscillators. Eur. Phys. J. Special Topics 2008;165:137-149.

[11] Ruan Y, Liu N, Priori SG. Sodium channel mutations and arrhythmias. Nat. Rev. Cardiol. 2009;6:337-348.

[12] Randall AD, Booth C, Brown JT. Age-related changes to Na^+ channel gating contribute to modified intrinsic neuronal excitability. Neurobiology of Aging 2012;33:2715–20.

[13] Cabo C, Pertsov AM, Baxter WT, Davidenko JM, Gray RA, Jalife J. Wave-front curvature as a cause of slow conduction and block in isolated cardiac muscle. Circulation Research 1994, 75:1014-1028.

[14] Berenfeld O, Zaitsev AV, Mironov SF, Pertsov AM, Jalife J. Frequency-Dependent Breakdown of Wave Propagation Into Fibrillatory Conduction Across the Pectinate Muscle Network in the Isolated Sheep Right Atrium. Circ Res 2002;90:1173-1180.

Address for correspondence:

Claudia Lenk
FG Physikalische Chemie (IfCB)
Technische Universität Ilmenau
Weimarer Strasse 25, 98693 Ilmenau
claudia.lenk@tu-ilmenau.de